Scaling of the H-mode electron separatrix density based on engineering parameters from C-Mod, AUG and JET data

D. Silvagni[1], O. Grover[1], A. Stagni[2], J. W. Hughes[3], M. A. Miller[3], B. Lomanowski[4], G. Ciraolo[5], W. Dekeyser[6], M. Dunne[1], T. Eich[7], L. Frassinetti[8], C. Giroud[9], T. Happel[1], I. Jepu[9], A. Kallenbach[1], A. Kirjasuo[10], A. Kuang[7], F. Latini[11], T. Luda[1], D. Moulton[9], O. Pan[1], C. Perez von Thun[12], T. Pütterich[1], S. A. Silburn[9], H. J. Sun[9], H. Zohm[1], the ASDEX Upgrade team[a], JET contributors[b] and the EUROfusion tokamak exploitation team[c]

[1]*Max-Planck-Institut für Plasmaphysik, 85748 Garching, Germany* [2]*Consorzio RFX, Corso Stati Uniti 4, 35127 Padova, Italy* [3]*MIT Plasma Science and Fusion Center, Cambridge, MA, USA* [4]*Oak Ridge National Laboratory, Oak Ridge, TN 37831-6169, USA* [5]*IRFM, CEA, St. Paul-Lez-Durance, France* [6]*KU Leuven, Department of Mechanical Engineering, Celestijnenlaan 300A, 3001 Leuven, Belgium* [7]*Commonwealth Fusion Systems, Devens, Massachusetts 01434, USA* [8]*Division of Electromagnetic Engineering and Fusion Science, KTH Royal Institute of Technology, Stockholm, Sweden* [9]*UKAEA, Culham Science Centre, Abingdon, OX14 3DB, UK* [1]*0VTT, PO Box 1000, FI-02044 VTT Espoo, Finland* [11] *Università della Tuscia, Dipartimento di Economia, Ingegneria, Società e Impresa (DEIM), 01100 Viterbo, Italy* [12]*Institute of Plasma Physics and Laser Microfusion, Hery 23, 01-497 Warsaw, Poland* [a]*See author list of H. Zohm, 2024 Nucl. Fusion 64 112001* [b]*See author list of C. F. Maggi, 2024 Nucl. Fusion 64 112012* [c]*See author list of E. Joffrin, 2024 Nucl. Fusion 64 112019*

E-mail: davide.silvagni@ipp.mpg.de

The separatrix electron density $n_{e,\text{sep}}$ is a critical plasma parameter that affects H-mode confinement, detachment achievement, ELM avoidance and sets a limit to H-mode operation. Therefore, quantitative prediction of $n_{e,\text{sep}}$ is essential for evaluating a core-edge integrated scenario solution in next-step devices. In this work, a scaling of the H-mode electron separatrix density $n_{e,\text{sep}}$ is presented, using data from Alcator C-Mod, ASDEX Upgrade and JET tokamaks with closed divertor configuration [1]. Regression analysis reveals that the plasma minor radius, a_geo, is the primary scaling parameter, with $n_{e,\text{sep}}$ decreasing as a_geo increases (see Fig. 1). This result is consistent with the 2-point model, which predicts $n_{e,\text{sep}} \propto a_\text{geo}^{-5/14}$. The key driver of this trend is the longer SOL connection length $L_{||}$ ($\propto a_\text{geo}$) which decreases $n_{e,\text{sep}}$. This finding has significant implications for the design of a fusion power plant. For the same target conditions (which are dictated by the divertor neutral pressure, $p_{0,\text{div}}$) and for the same divertor geometry, increasing the machine size leads to a lower upstream $n_{e,\text{sep}}$, which is typically associated with higher H-mode confinement [2] and lower disruption risk [3]. Therefore, for the same divertor geometry, increasing the machine size could facilitate achievement of a core-edge integrated scenario. However, it should be noted that the physics parameter driving $n_{e,\text{sep}}$ down is the SOL connection length; Therefore, use of alternative divertor configurations which prolong $L_{||}$ for the same machine size may offer a compact design solution while attaining power-plant relevant core conditions.

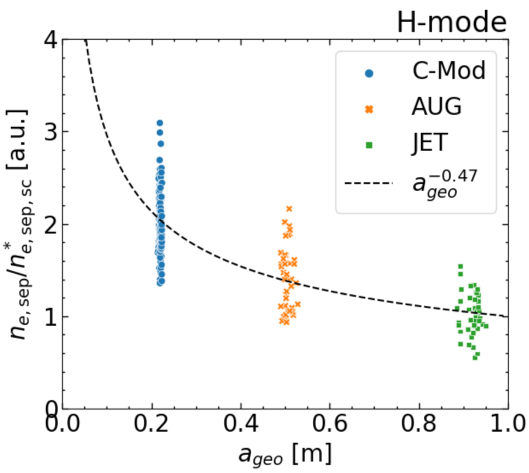

Figure 1: Experimental $n_{e,\text{sep}}$ normalized by $n^*_{e,\text{sep,sc}}$ (i.e. Eq. 1 without the a_geo dependence) vs. the geometrical plasma minor radius for C-Mod, AUG and JET.

The assembled multi-machine database consists of H-mode discharges with and without ELMs, in favorable configuration and with closed divertor geometry. The separatrix parameters have been evaluated by fitting edge Thomson scattering data with the same function and by consistently applying (inter-ELM) SOL power balance in each device. Details of the analysis technique can be found in Ref. [1]. The regression variables used in this work are I_p (MA), B_t (T), a_geo (m), $p_{0,\text{div}}$ (Pa), i.e. the divertor neutral pressure measured by baratrons in the subdivertor region, and $P_\text{SOL}/R_\text{geo}$ (MW/m), where P_SOL is the power entering the scrape-off layer. A power law regression of this database using a generalized linear model with Gaussian likelihood and the logarithmic link function yields:

$$n_{e,\text{sep,sc}} = C_\text{tok} p_{0,\text{div}}^{0.20} I_p^{0.03} B_t^{-0.26} \left(\frac{P_\text{SOL}}{R_\text{geo}}\right)^{0.19} a_\text{geo}^{-0.47}, \tag{1}$$

with $R^2 = 0.91$ and normalized root mean square error NRMSE = 19 %. A tokamak-specific multiplication constant, C_{tok}, is used, which is determined through regression analysis. The values obtained are 6.3 for C-Mod, 2.0 for AUG, and 3.0 for JET. These constants are introduced to facilitate comparison with the two-point model, as discussed later. As already mentioned, the primary scaling parameter is a_{geo}, followed by the on-axis magnetic field, which also reduces $n_{e,\text{sep}}$ when increased. The two parameters that drive an increase in $n_{e,\text{sep}}$ are the divertor neutral pressure and $P_{\text{SOL}}/R_{\text{geo}}$, with almost identical exponent (~ 0.2). The dependence on $p_{0,\text{div}}$ is similar to the one found analyzing single machines [4, 1], with a slightly lower exponent. A similar dependence between $n_{e,\text{sep}}$ and $p_{0,\text{div}}$ has been found in SOLPS gas scan simulations of an AUG H-mode case (see Fig. 2) and in recent SOLPS-ITER simulations for ITER Q=10 baseline scenario [5]. Interestingly, the regression finds no significant dependence of $n_{e,\text{sep}}$ on the plasma current.

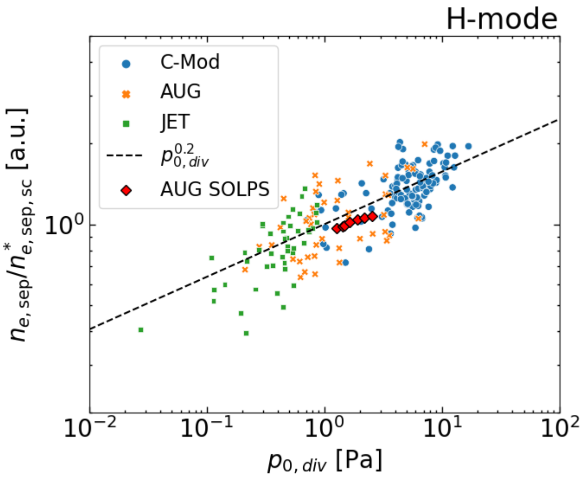

Figure 2: Experimental $n_{e,\text{sep}}$ normalized by $n^*_{e,\text{sep,sc}}$ (i.e. Eq. 1 without the $p_{0,\text{div}}$ dependence) vs. the divertor neutral pressure for C-Mod, AUG and JET data. Results of a SOLPS gas scan for an AUG H-mode case are plotted with red diamonds.

To interpret these results, the basic equations of the 2-point model are solved to express $n_{e,\text{sep}}$ as a function of similar parameters, giving:

$$n_{e,\text{sep,2pt}} = C_{\text{2pt}} p_{0,\text{div}}^{1/2} I_p^{1/14} B_t^{-1/14} \left(\frac{P_{\text{SOL}}}{R_{\text{geo}} \lambda_q} \right)^{3/14} a_{\text{geo}}^{-5/14}, \tag{2}$$

where λ_q is the power decay length mapped to the outer midplane and C_{2pt} is a constant that depends on various general and machine-specific parameters. The exponents of I_p, $P_{\text{SOL}}/R_{\text{geo}}$ and a_{geo} are similar to those found with regression analysis. However, the exponents of $p_{0,\text{div}}$ and B_t are somewhat stronger and weaker in magnitude, respectively, than those found in the regression. This discrepancy could stem from additional hidden dependencies of the loss factors contained in C_{2pt} [4] and of λ_q on these parameters. Nevertheless, the good agreement between the regression result and the 2-point model equation suggests that recycling at the divertor target influences the upstream $n_{e,\text{sep}}$ in the analyzed dataset. In particular, the a_{geo} dependence in Eq. 2 can be attributed to the connection length between the target and the outer midplane, $L_{||}$ ($\propto a_{\text{geo}}$). A longer $L_{||}$ leads to a higher upstream $T_{e,\text{sep}}$ due to electron conduction, which, in turn, reduces $n_{e,\text{sep}}$ to maintain pressure balance along the magnetic field line. With this simple model in mind, Eq. 1 and 2 can be used to guide integrated modeling and next-step machine design. Of particular importance for extrapolation purposes is the comparison of the two multiplication constants, C_{tok} and C_{2pt}. Such a comparison is challenging because $p_{0,\text{div}}$ is measured at different locations in each machine [1], introducing an additional geometric factor related to the specific device engineering. To address this issue, SOLPS and EDGE2D EIRENE simulations are employed to establish a relationship between the neutral pressure at the measurement location and at the outer target in each machine.

References

[1] D. Silvagni et al., Nucl. Materials and Energy **42**, 101867 (2025)
[2] L. Frassinetti et. al, Nucl. Fusion **61**, 126054 (2021)
[3] T. Eich et al., Nucl. Fusion **61**, 086017 (2021)
[4] A. Kallenbach et al., Plasma Phys. Control. Fusion **60**, 045006 (2018)
[5] A. A. Pshenov et al., Nucl. Materials and Energy **42** (2025) 101851